

# Impact of threading dislocation density on the lifetime of InAs quantum dot lasers on Si

Daehwan Jung,<sup>1,a)</sup> Robert Herrick,<sup>2</sup> Justin Norman,<sup>3</sup> Katherine Turnlund,<sup>1</sup> Catherine Jan,<sup>2</sup> Kaiyin Feng,<sup>4</sup> Arthur C. Gossard,<sup>1,3,4</sup> and John E. Bowers<sup>1,3,4</sup>

<sup>1</sup>Institute for Energy Efficiency, University of California, Santa Barbara, California 93106, USA

<sup>2</sup>Intel Corporation, Santa Clara, California 95054, USA

<sup>3</sup>Materials Department, University of California, Santa Barbara, California 93106, USA

<sup>4</sup>Department of Electrical and Computer Engineering, University of California, Santa Barbara, California 93106, USA

(Received 16 February 2018; accepted 2 April 2018; published online 13 April 2018)

We investigate the impact of threading dislocation density on the reliability of 1.3  $\mu\text{m}$  InAs quantum dot lasers epitaxially grown on Si. A reduction in the threading dislocation density from  $2.8 \times 10^8 \text{ cm}^{-2}$  to  $7.3 \times 10^6 \text{ cm}^{-2}$  has improved the laser lifetime by about five orders of magnitude when aged continuous-wave near room temperature (35 °C). We have achieved extrapolated lifetimes (time to double initial threshold) more than  $10 \times 10^6 \text{ h}$ . An accelerated laser aging test at an elevated temperature (60 °C) reveals that p-modulation doped quantum dot lasers on Si retain superior reliability over unintentionally doped ones. These results suggest that epitaxially grown quantum dot lasers could be a viable approach to realize a reliable, scalable, and efficient light source on Si. Published by AIP Publishing. <https://doi.org/10.1063/1.5026147>

III/V lasers epitaxially grown on Si have been actively studied for their potential applications such as monolithic integration of large-scale Si electronics and various III/V photonic devices.<sup>1</sup> From a material standpoint, growth of III/V layers on Si faces two major challenges. The large lattice mismatch ( $\sim 4\%$ ) and heterovalent polar/non-polar interface between III/V and Si result in high threading dislocation density (TDD) and antiphase domains (APDs), respectively.<sup>2</sup> The use of  $4^\circ$ – $6^\circ$  offcut Si substrates and a combination of thermal cycle annealing and dislocation filter layers have effectively circumvented formation of APDs and reduced TDDs in GaAs buffers below  $\sim 1 \times 10^6 \text{ cm}^{-2}$ .<sup>3</sup> Although GaAs quantum well (QW) lasers grown on the high quality GaAs/Si templates showed impressive performance in terms of low threshold current density ( $\sim 600 \text{ A/cm}^2$ ) after more than a decade of research, they failed to attain sufficient lifetimes to be fully considered for commercial applications.<sup>4</sup> In those lasers, a sudden failure was observed typically within hundreds of hours of room-temperature operation due to formation of dark-line defects,<sup>5,6</sup> and the most prolonged lifetime reported among GaAs-based QW lasers on Si is merely  $\sim 200 \text{ h}$ .<sup>7</sup>

Recently, replacing the QW active region with InAs quantum dots (QDs) in the GaAs-based lasers grown on Si has demonstrated considerable advances in laser performance as well as reliability. Liu *et al.* reported an extrapolated laser lifetime (time of a doubling initial threshold) up to  $\sim 4600 \text{ h}$  from QD lasers grown on Ge/Si templates after a 2700 h aging test at 30 °C.<sup>8</sup> Also, Chen *et al.* demonstrated one broad-area QD laser with an  $\sim 100\,000 \text{ h}$  extrapolated lifetime by aging it at 26 °C under a constant current injection of  $1.75 \times$  initial threshold.<sup>9</sup> Both studies showed no abrupt failure, excluding the possibility of dark-line defects or catastrophic optical damage on the cavity facets. It has been thought that effective carrier

localization in QDs considerably improved the laser reliability over QW Si lasers by suppressing growths of (100) dark-line defects, which were commonly observed in GaAs-based lasers.<sup>10</sup> Instead, recombination enhanced dislocation climb (REDC) was identified as the dominant degradation mechanism of the gradual degradation process.<sup>8,11</sup> Therefore, a rigorous study on the impact of the TDD in QD lasers on Si is necessary to realize commercially viable III/V light sources monolithically integrated on Si. Moreover, aging QD Si lasers at elevated temperatures has never been reported but is important because real-world applications require stable long-term operation above room temperature without an additional active cooling system.

Here, we report the lifetimes of the QD lasers epitaxially grown on three different GaAs/Si templates with various TDDs. The extrapolated lifetimes from the QD lasers grown on the  $7.3 \times 10^6 \text{ cm}^{-2}$  template are more than  $10 \times 10^6 \text{ h}$  while those on the high TDD template are limited to  $\sim 500 \text{ h}$  of lifetime. A similar trend in the laser slope efficiencies was observed during the aging test. Moreover, QD Si lasers with a low TDD were aged at an elevated temperature (60 °C) to investigate the temperature effects, and p-modulation doped QD lasers demonstrated an extrapolated lifetime of  $\sim 65\,000 \text{ h}$ .

All laser samples were grown in a solid-source molecular beam epitaxy (MBE) chamber. Three different GaAs buffer layers were first grown on GaP/Si substrates. More information about the starting GaP/Si wafers can be found elsewhere.<sup>12</sup> For Generation-I lasers (Gen-I), a two-step growth temperature technique was applied for the GaAs buffer layer. The Gen-II template added four cycles of thermal cycle annealing. For the Gen-III buffer, InGaAs/GaAs strained layer superlattices were inserted as dislocation filter layers to further reduce TDD in addition to the two-step growth and thermal cycle annealing.<sup>13</sup> Then, the samples were removed from the MBE chamber to characterize the TDD using the electron channeling contrast imaging (ECCI) technique.<sup>13</sup> Figures

<sup>a)</sup>E-mail: daehwan.jung.ucs@gmail.com

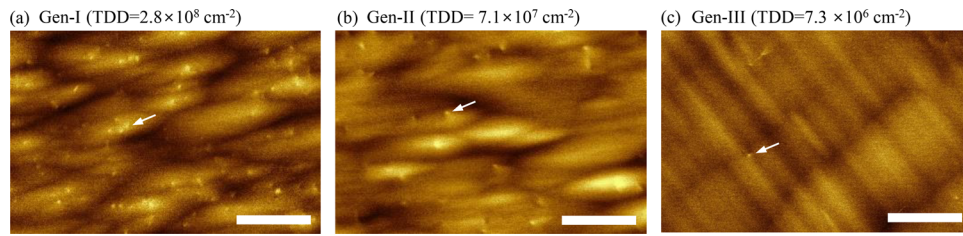


FIG. 1. Electron channeling contrast images on GaAs buffers grown on Si. (a) Gen-I template, (b) Gen-II template, and (c) Gen-III template. Arrows indicate a single threading dislocation observed on the surface. The scale bar is 2  $\mu\text{m}$ .

1(a)–1(c) show representative ECCI images from each GaAs/Si template. We have surveyed an area of  $\sim 180 \mu\text{m}^2$ ,  $\sim 580 \mu\text{m}^2$ , and  $\sim 3000 \mu\text{m}^2$  for the Gen-I, II, and III buffer, respectively. The TDD for each buffer is  $2.8 \times 10^8 \text{ cm}^{-2}$ ,  $7.1 \times 10^7 \text{ cm}^{-2}$ , and  $7.3 \times 10^6 \text{ cm}^{-2}$ . More detailed defect characterizations by ECCI can be found elsewhere.<sup>13</sup> Then, the templates were loaded back to the MBE chamber to grow GaAs/AlGaAs graded-index separate confinement heterostructure lasers.<sup>14</sup> The Gen-I and Gen-II lasers have 7 layers of p-modulation doped ( $p = 5 \times 10^{17} \text{ cm}^{-3}$ ) QD layers, while Gen-III lasers have unintentionally doped (UID) 5 QD layers in an attempt to achieve low threshold currents at room temperature. The samples were fabricated into narrow ridge-waveguide lasers via standard photolithography. The lasers presented here have similar sizes in ridge widths from 3 to 5  $\mu\text{m}$  and cavity lengths from 1000 to 1641  $\mu\text{m}$  to avoid additional impacts on the reliability coming from a different device dimension. One facet of the lasers was coated with a high-reflectivity film ( $\sim 99\%$ ). For the reliability test, the laser chips were wirebonded onto AlN aging carriers and aged at Intel Corporation. The QD lasers were stressed at 35 °C or 60 °C under continuous-wave (CW) operation, and the driving current was set at about  $2 \times$  initial threshold current of each laser. Light-current-voltage (LIV) sweeps were periodically performed to monitor the laser performance.

Threshold currents were extracted from the light-current (LI) curves, and they are displayed in Fig. 2. The Gen-I lasers revealed rapid sub-linear increases in the threshold currents. With a criterion for failure as 100% increase in threshold current,<sup>8</sup> one Gen-I laser (red circle) has a lifetime of 355 h while the other (black circle) is expected to double the initial threshold in 1097 h using a non-linear model (black dashed curve).<sup>8</sup> The Gen-II and Gen-III lasers, which were grown on the GaAs/Si template with a TDD of  $7.1 \times 10^7 \text{ cm}^{-2}$  and  $7.3 \times 10^6 \text{ cm}^{-2}$ , revealed improved reliability with slower increases in the threshold current over the aging periods as shown in Figs. 2(b) and 2(c). It should be noted that the Gen-III lasers operated with almost no degradation after the initial  $\sim 200$  h of aging at 35 °C, all of which resulted in lifetimes more than  $10 \times 10^6$  h. Figure 2(d) shows a lifetime extraction from one of the Gen-III lasers using the non-linear fit (blue curve).<sup>8</sup> Some Gen-III lasers showed faster degradation rates than the others because of higher initial threshold current densities caused by imperfect device fabrication and handling (see Fig. S1 in the [supplementary material](#)).

Figure 3 summarizes the extrapolated lifetimes of various QD lasers grown on the three different GaAs/Si templates and the lasers grown on the Ge/Si template from Ref. 8. The QD density (QDD) per layer of the Gen-I lasers is  $\sim 3 \times 10^{10} \text{ cm}^{-2}$

while that of the Gen-II and III is  $\sim 5 \times 10^{10} \text{ cm}^{-2}$ . A good linear relationship between the extrapolated laser lifetimes and TDD can be found even though the number of QD layers, device dimension, and aging conditions are slightly different, indicating that the rate of laser degradation is mainly determined by the relative density of QDs over threading dislocations (TDs) in the active region. Note that the typical carrier migration length in the InAs/InGaAs QD system is around

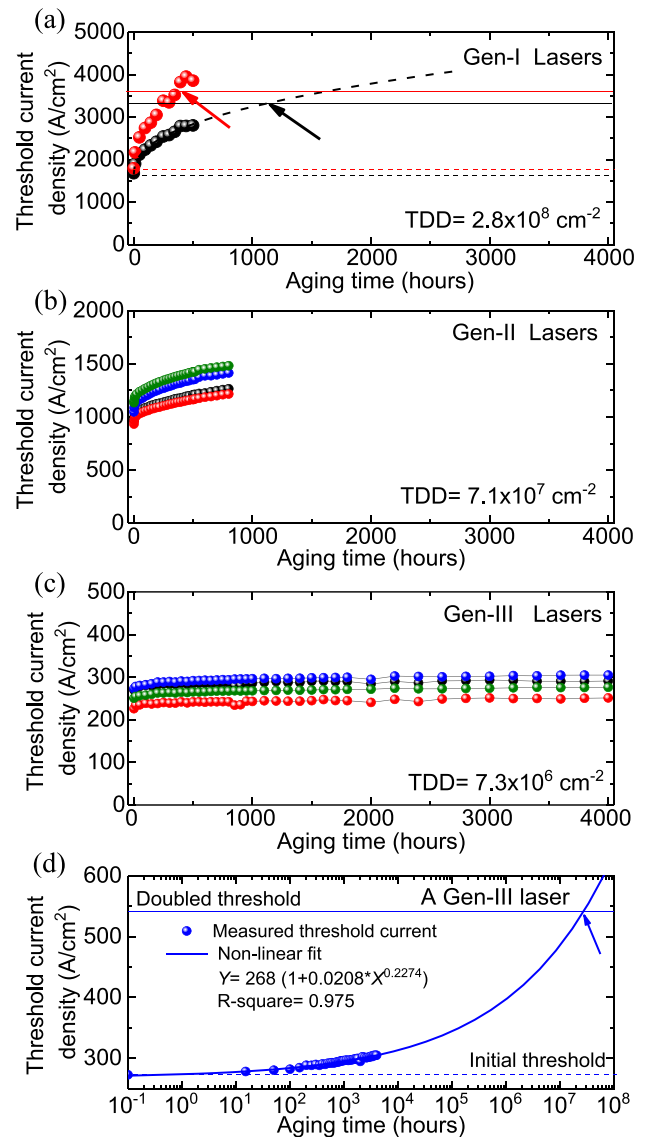


FIG. 2. Continuous-wave threshold current density versus aging time from (a) two Gen-I lasers, (b) four Gen-II lasers, (c) four Gen-III lasers at 35 °C, and (d) one of the Gen-III lasers. The dotted lines and solid lines in (a) and (d) indicate the initial and doubled threshold current densities, respectively.

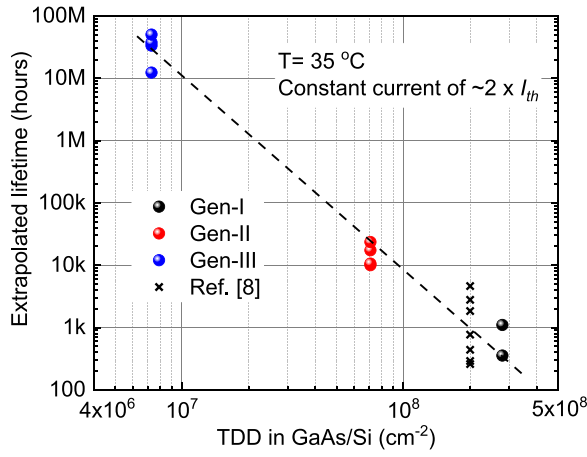


FIG. 3. Extrapolated quantum dot laser lifetime versus the threading dislocation density. Lasers from Ref. 8 were aged at 30 °C. The dashed line is a linear fit.

$\sim 1 \mu\text{m}$  near room temperature.<sup>15–17</sup> In the case of the Gen-I lasers where the TDD is  $2.8 \times 10^8 \text{ cm}^{-2}$ , there are roughly  $\sim 3$  TDs in  $1 \mu\text{m}^2$ . Therefore, all the QDs are potentially under the influence of nearby TDs for the non-radiative recombination process. However, in the Gen-III lasers, for instance, there are only  $\sim 7$  TDs in  $100 \mu\text{m}^2$ , and the affecting area by the TDs would be  $7 \times \pi r^2 \approx 22 \mu\text{m}^2$ , where  $r$  is the carrier migration length. Hence, nearly 80% of the QDs in the Gen-III lasers is safe from the potential influence of TDs. This effectively increases the laser injection efficiency and also reduces the rate of the REDC process, eventually enabling the superior reliability in the Gen-III lasers.<sup>18</sup>

Another important parameter to study is the slope efficiency changes above threshold since some applications may require high output powers more than a couple mW. Figure 4 shows that the slope efficiencies of the Gen-I lasers dropped to almost half of the initial values during the 500 h aging. However, the slope efficiencies of the Gen-III lasers decreased by only  $\sim 8\%$  during the entire 4000 h aging period. Figure 5 shows the average bias current increases to produce certain output powers during the aging tests; 2 mW for Gen-I and 10 mW for Gen-II and Gen-III. Using a power

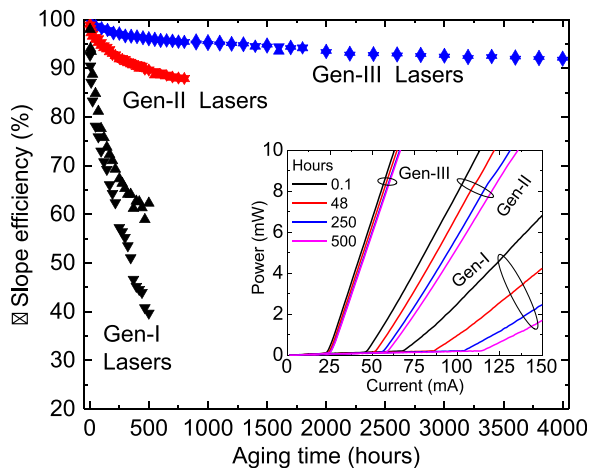


FIG. 4. Changes in slope efficiency versus aging time at 35 °C. Two representative lasers are shown from each template. The inset shows LI curves taken from a representative laser from each sample during the initial 500 h aging.

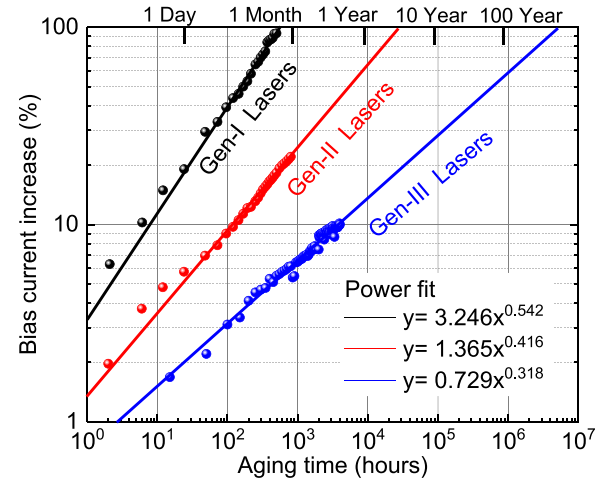


FIG. 5. Bias current increase versus aging time. Solid lines are a power fit. R-squared values are 0.995, 0.996, and 0.978 for Gen-I, Gen-II, and Gen-III, respectively.

fit ( $y = a \times t^b$ ), we have also extracted times of a doubling of the bias current and have achieved  $\sim 500 \text{ h}$ ,  $\sim 27\,000 \text{ h}$ , and  $\sim 5 \times 10^6 \text{ h}$  for Gen-I, Gen-II, and Gen-III, respectively. These results demonstrate that the Gen-III lasers grown on the low TDD are able to maintain the low threshold current as well as the high slope efficiency.

Practical applications of QD lasers on Si such as data centers or on-chip optical interconnects may require long-term operation at an elevated temperature. To study reliability above room temperature, two UID Gen-III lasers have been aged at 60 °C and periodic LIV sweeps were taken at 35 °C to investigate their accelerating degradation. The aging current (100 mA) was set at  $2 \times$  initial threshold currents (44 mA and 49 mA) at 60 °C. Unlike the 35 °C aging result, we have observed faster degradation rates in both lasers, as shown in Fig. 6(a). The laser lifetimes of the two lasers are  $\sim 2500 \text{ h}$

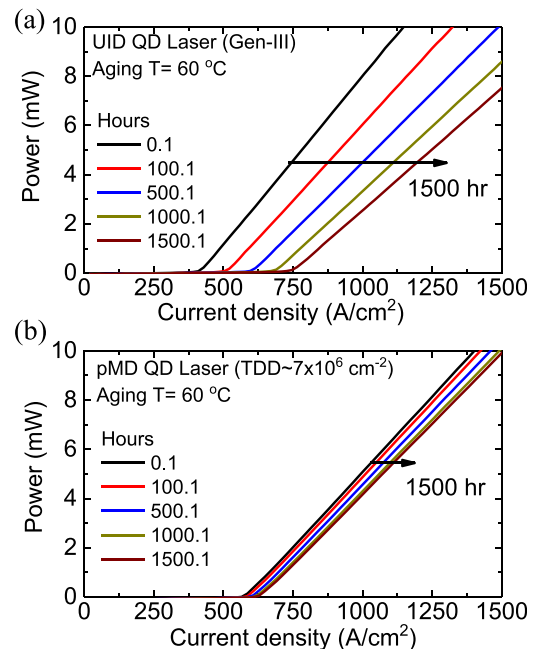


FIG. 6. LI curves from 60 °C aging test of (a)  $3.5 \times 1633 \mu\text{m}$  UID QD laser and (b)  $3.5 \times 1364 \mu\text{m}$  p-doped QD laser. LIV sweeps were taken at 35 °C after cooling from aging temperature.



from the 60 °C aging condition. We believe that the increased aging current density and temperature have accelerated the device degradation speed. It is well-known that p-modulation doped QD lasers possess higher differential gain and better thermal performance with higher characteristic temperature ( $T_0 \sim 100$  K) than the UID lasers ( $T_0 \sim 30$  K) (see Fig. S2 in the [supplementary material](#) for T-dependent threshold current densities).<sup>19</sup> Figure 6(b) shows 35 °C LI curves from one of the p-doped QD lasers ( $p = 1 \times 10^{18} \text{ cm}^{-3}$ , TDD  $\sim 7 \times 10^6 \text{ cm}^{-2}$ ) that has been aged at 60 °C and 80 mA driving current. The laser initial threshold current was 37.5 mA at 60 °C. The extrapolated lifetimes (doubling the initial threshold) of the p-modulation doped lasers are  $\sim 65$  000 h.

It should be mentioned that the aging current density of the UID and p-doped QD lasers is nearly the same,  $\sim 1700 \text{ A/cm}^2$  at 60 °C. Therefore, other positive effects occur from p-doping in the QD laser reliability above room temperature. Typically, p-doped QD lasers tend to have a lower threshold current over UID lasers from  $\sim 40$  °C and above even with the increased optical internal loss due to inter-valence band absorption.<sup>19,20</sup> This means that the faster carrier transfers from the GaAs barrier to the ground-state energies in p-doped QDs preserve the high injection efficiency and high differential gain at elevated temperatures,<sup>21</sup> whereas UID lasers lack nearby holes due to thermalization. From a reliability point of view, the quicker carrier transfer leads to a faster carrier capture to p-doped QDs, which can reduce the number of free carriers available for trap-assisted non-radiative recombination by TDs.

Compared to heterogeneously bonded III-V Si lasers that have demonstrated nearly degradation-free operation at 85 °C,<sup>22</sup> further advancements in InAs QD/GaAs buffer material quality and device design are required to be fully considered for practical applications. For instance, misfit dislocations running in the QD active region may be more effective sources for degradation than TDs when TDD is low at  $\sim 5 \times 10^6 \text{ cm}^{-2}$ . Therefore, a reduced number of QD layers or a strain-balanced QD active region needs to be studied to avoid misfit dislocations. Also, indium doping in the active region or in the core region may be benefiting laser reliability by pinning dislocations as already seen in InP-based lasers.<sup>23,24</sup> In terms of device design, residual thermal stress in GaAs on Si ( $\sim 250$  MPa) that is detrimental to device reliability by promoting dislocation motion<sup>25</sup> could be relieved by forming high aspect-ratio laser structures such as micro-ring lasers. Finally, further optimizations on the laser growth conditions may also improve reliability by reducing the number of point defects such as vacancies and interstitials.

In conclusion, we have investigated the impact of threading dislocation density on the reliability of 1.3  $\mu\text{m}$  InAs quantum dot lasers epitaxially grown on Si. The aging results at 35 °C have shown that reducing the dislocation density from  $2.8 \times 10^8 \text{ cm}^{-2}$  to  $7.3 \times 10^6 \text{ cm}^{-2}$  has improved the laser lifetime (time to double initial threshold current) from a few thousand hours to more than  $10 \times 10^6$  h. Lowering the dislocation density also helped in maintaining the slope efficiencies of the lasers during the aging test. While elevating the aging temperature to 60 °C has significantly decreased the lifetimes of the undoped lasers, p-modulation doped quantum dot lasers demonstrated viability

for practical applications above room temperature. With the rapid progress in the reliability of the epitaxially grown quantum dot Si lasers, this study shows a promising pathway for reliable, efficient, and scalable light sources on Si substrates.

See [supplementary material](#) for extrapolated lifetimes of Gen-III lasers vs. threshold current densities and temperature-dependent threshold current density data.

This research was supported by Advanced Research Projects Agency-Energy (ARPA-E) No. DE-AR000067. We are grateful to Kurt Olsson and John English for their assistance in MBE maintenance and Alan Liu, Kei May Lau, Chris Palmström, and Kunal Mukherjee for fruitful discussions. We are also thankful to Alfredo Torres for wirebonding and Neil Caranto for reliability test results.

- <sup>1</sup>T. Windhorn, G. Metzger, B. Tsaur, and J. Fan, *Appl. Phys. Lett.* **45**, 309 (1984).
- <sup>2</sup>W. Wang, *Appl. Phys. Lett.* **44**, 1149 (1984).
- <sup>3</sup>M. Yamaguchi, T. Nishioka, and M. Sugo, *Appl. Phys. Lett.* **54**, 24 (1989).
- <sup>4</sup>M. Groenert, C. Leitz, A. Pitera, V. Yang, H. Lee, R. Ram, and E. Fitzgerald, *J. Appl. Phys.* **93**, 362 (2003).
- <sup>5</sup>Y. Hasegawa, T. Egawa, T. Jimbo, and M. Umeno, *Jpn. J. Appl. Phys.* **34**, 2994 (1995).
- <sup>6</sup>T. Egawa, T. Jimbo, Y. Hasegawa, and M. Umeno, *Appl. Phys. Lett.* **64**, 1401 (1994).
- <sup>7</sup>Z. Kazi, P. Thilakan, T. Egawa, M. Umeno, and T. Jimbo, *Jpn. J. Appl. Phys.* **40**, 4903 (2001).
- <sup>8</sup>A. Liu, R. Herrick, O. Ueda, P. Petroff, A. Gossard, and J. Bowers, *IEEE J. Sel. Top. Quantum Electron.* **21**, 1900708 (2015).
- <sup>9</sup>S. M. Chen, W. Li, J. Wu, Q. Jiang, M. C. Tang, S. Shutts, S. N. Elliott, A. Sobiesierski, A. J. Seeds, I. Ross, P. M. Smowton, and H. Y. Liu, *Nat. Photonics* **10**, 307 (2016).
- <sup>10</sup>S. Yellen, A. Shepard, R. Dalby, J. Baumann, H. Serreze, T. Guido, R. Soltz, K. Bystrom, C. Harding, and R. Waters, *IEEE J. Quantum Electron.* **29**, 2058 (1993).
- <sup>11</sup>L. Kimerling, *Solid-State Electron.* **21**, 1391 (1978).
- <sup>12</sup>I. Nemeth, B. Kunert, W. Stolz, and K. Volz, *J. Cryst. Growth* **310**, 1595 (2008).
- <sup>13</sup>D. Jung, P. Callahan, B. Shin, K. Mukherjee, A. Gossard, and J. Bowers, *J. Appl. Phys.* **122**, 225703 (2017).
- <sup>14</sup>D. Jung, J. Norman, M. Kennedy, C. Shang, B. Shin, Y. Wan, A. Gossard, and J. Bowers, *Appl. Phys. Lett.* **111**, 122107 (2017).
- <sup>15</sup>D. Popescu, P. Eliseev, A. Stintz, and K. Malloy, *J. Appl. Phys.* **94**, 2454 (2003).
- <sup>16</sup>A. Sobiesierski, D. Naidu, P. Smowton, and A. Belyanin, "Novel in-plane semiconductor lasers X," *Proc. SPIE* **7953**, 795306 (2011).
- <sup>17</sup>S. Moore, L. O'Faolain, M. Cataluna, M. Flynn, M. Kotlyar, and T. Krauss, *IEEE Photonics Technol. Lett.* **18**, 1861 (2006).
- <sup>18</sup>D. Jung, Z. Zhang, J. Norman, R. Herrick, M. Kennedy, P. Patel, K. Turnlund, C. Jan, Y. Wan, A. Gossard, and J. Bowers, *ACS Photonics* **5**, 1094 (2018).
- <sup>19</sup>R. Alexander, D. Childs, H. Agarwal, K. Groom, H. Liu, M. Hopkinson, R. Hogg, M. Ishida, T. Yamamoto, M. Sugawara, Y. Arakawa, T. Badcock, R. Royce, and D. Mowbray, *IEEE J. Quantum Electron.* **43**, 1129 (2007).
- <sup>20</sup>Y. Jang, T. Badcock, D. Mowbray, M. Skolnick, J. Park, D. Lee, H. Liu, M. Hopkinson, R. Hogg, and A. Andreev, *Appl. Phys. Lett.* **93**, 101903 (2008).
- <sup>21</sup>J. Siegert, S. Marcinkevicius, and Q. Zhao, *Phys. Rev. B* **72**, 085316 (2005).
- <sup>22</sup>S. Srinivasan, N. Julian, J. Peters, D. Liang, and J. Bowers, *IEEE J. Sel. Top. Quantum Electron.* **19**, 1501305 (2013).
- <sup>23</sup>H. Wang, A. Hopgood, and G. Ng, *J. Appl. Phys.* **81**, 3117 (1997).
- <sup>24</sup>R. Waters, *Prog. Quantum Electron.* **15**, 153 (1991).
- <sup>25</sup>S. Sakai and N. Wada, *Fiber Integr. Opt.* **13**, 31 (1994).